

Accurate cw Measurements of Optical Second-Harmonic Generation in Ammonium Dihydrogen Phosphate and Calcite*

J. E. BJORKHOLM† AND A. E. SIEGMAN

Division of Applied Physics and Department of Electrical Engineering, Stanford University, Stanford, California

(Received 1 September 1966)

Optimally focused cw gas-laser beams were used to make an accurate absolute measurement of optical second-harmonic generation (SHG) in ammonium dihydrogen phosphate (ADP) and accurate relative measurements of the higher order quadrupole-type SHG and electric-field-induced SHG in calcite. The result of the first set of experiments was $d_{36}(\text{ADP}) = 1.38 \times 10^{-9}$ esu $\pm 16\%$, in excellent agreement with the value determined by Francois using unfocused beams. This agreement demonstrates that focused laser beams can be used to make accurate measurements of crystal nonlinearities, and it provides further evidence that the value of d_{36} in potassium dihydrogen phosphate (KDP), normally taken as the standard nonlinearity, is considerably smaller than the value usually quoted. The nonlinearity describing quadrupole-type SHG in calcite was found to be $2.8 \times 10^{-4} d_{36}(\text{ADP}) \pm 14\%$, and that for electric-field-induced SHG was $2.1 \times 10^{-5} d_{36}(\text{ADP}) \pm 24\%$. The second-harmonic power from calcite could not have been measured without the enhancements available from focusing. A displacement of the parabolic curve of second-harmonic power as a function of the applied electric field was noted, and it was shown that this shift was not caused by inhomogeneous applied electric fields. The very small induced birefringence in calcite which depends quadratically upon the applied electric field was also measured.

I. INTRODUCTION

THE most accurate absolute measurements of nonlinear optical effects have been made using the light beams from cw gas lasers. The reason for this accuracy is that the mode structure of a gas laser can be accurately controlled; knowledge of the mode structure makes it possible to carry out detailed calculations. There is a major disadvantage, however. The optical powers available from gas lasers are orders of magnitude smaller than the powers obtained from pulsed solid-state lasers and hence the nonlinear effects are much weaker and more difficult to observe. Thus, the technique of index matching^{1,2} is usually employed in order to measure optical second-harmonic generation on a cw basis. In order to further improve the conversion efficiencies, the laser beam can be focused inside the nonlinear medium. The case of optical second-harmonic generation (SHG) by a focused Gaussian laser beam in double-refractive, index-matching crystals has been analyzed in a previous paper by one of the authors.³ It was shown that for a given nonlinear crystal there is an optimum degree of focusing which yields a maximum amount of second-harmonic power for fixed laser beam power. This maximum second-harmonic power can be several orders of magnitude larger than the power generated by a collimated or unfocused beam. The purpose of this paper is to report accurate measurements of several nonlinearities associated with SHG in crystals of ammonium dihydrogen phosphate (ADP) and calcite. The experiments were carried out with

optimally focused beams from a He-Ne laser operating at 6328 Å in the lowest order transverse (Gaussian) mode.

In the first section of this paper we report the accurate absolute measurement of the nonlinear susceptibility tensor element d_{36} in ADP. In spite of the fact that there have been several previous absolute measurements of d_{36} in ADP and in potassium dihydrogen phosphate (KDP) made with unfocused laser beams,⁴⁻⁶ there were good reasons to repeat these measurements using optimally focused beams. First of all, the experiments reported in Ref. 3 only confirmed that the dependence of the second-harmonic power $P_{2\omega}$ upon the degree of focusing of the laser beam was as predicted by the calculations. In order to complete the verification of the theory, it is also necessary to show that the absolute value of $P_{2\omega}$ was in agreement with the calculations. Our measured value for d_{36} was found to be in excellent agreement with the accurate value determined by Francois⁶ in detailed experiments using unfocused beams. This agreement is the required further confirmation that the calculations carried out in Ref. 3 do accurately describe SHG in the focus of a Gaussian laser beam. In addition, the agreement of our measurements with those of Francois provides further evidence that the value for d_{36} in KDP is considerably smaller than the value usually quoted in the literature. These more accurate absolute values for d_{36} in ADP and their implications for d_{36} in KDP are important because these elements are often taken as standard nonlinearities against which other nonlinearities are compared in relative measurements.⁷

* This research was supported by the U. S. Air Force Office of Scientific Research Contract No. AF 49(638)-1525.

† Present address: Bell Telephone Laboratories, Murray Hill, New Jersey.

¹ J. A. Giordmaine, *Phys. Rev. Letters* **8**, 19 (1962).

² P. D. Maker, R. W. Terhune, M. Nisenoff, and C. M. Savage, *Phys. Rev. Letters* **8**, 21 (1962).

³ J. E. Bjorkholm, *Phys. Rev.* **142**, 126 (1966).

⁴ A. Ashkin, G. D. Boyd, and J. M. Dziedzic, *Phys. Rev. Letters* **11**, 14 (1963).

⁵ D. H. McMahon and A. R. Franklin, *Appl. Phys. Letters* **6**, 14 (1965).

⁶ G. E. Francois, *Phys. Rev.* **143**, 597 (1966).

⁷ R. C. Miller, D. A. Kleinman, and A. Savage, *Phys. Rev. Letters* **11**, 146 (1963).

The remainder of this paper is concerned with accurate cw measurements of the very weak SHG which occurs in crystals of calcite. Calcite has a center of inversion, and dipolar SHG (like that which occurs in ADP) cannot occur. Thus SHG in calcite is due to higher order nonlinearities and these effects are much weaker. They are so small, in fact, that we could not have measured them on a cw basis without the use of focused laser beams. In our experiments we measured quadrupole-type SHG and electric-field-induced SHG relative to the SHG obtained in crystals of ADP. These effects in calcite were first measured by Terhune, Maker, and Savage (TMS) using a pulsed ruby laser.⁸ Our experiments yield more accurate measurements of the two nonlinearities. The displacement of the parabolic curve of second-harmonic power as a function of the applied electric field mentioned by TMS was also noted in our experiments. Although the exact origin of the curve shift could not be determined from our measurements, it was ascertained that it was not due to inhomogeneous applied electric fields.⁹ Several other possible explanations for the curve shift are discussed. A measurement of the very small induced birefringence depending quadratically upon the applied electric field was also carried out.

II. MEASUREMENTS IN ADP

The basic experimental setup used in our measurements is shown in the schematic diagram of Fig. 1. The He-Ne laser was operated at 6328 Å in the lowest order transverse mode. A narrow-band interference filter, not shown in the diagram, was used to eliminate the fluorescence of the laser tube. Discussion of the experimental setup and the techniques used in the measurements will not be given here since they are the same as those described in Ref. 3. The discussion given here will concern itself with a description of the method used to measure the generated second-harmonic power on an absolute basis.

It is very difficult to calibrate a low level photomultiplier accurately in terms of absolute light power. In order to avoid this problem, the following technique was used to absolutely measure the second-harmonic power. The signal evoked in the detection system by the unknown amount of second-harmonic radiation was directly compared with the signal due to a known amount of light at the fundamental frequency impinging on the same photomultiplier, with all electronic adjustments remaining unchanged. Thus, the gains of the electronic apparatus and of the electron multiplication drop out of this comparison, leaving only the ratio of the sensitivities of the photomultiplier's photocathode at the two wavelengths. If this ratio (i.e., ratio of the

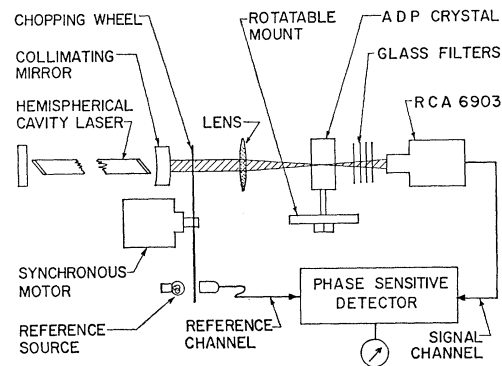


Fig. 1. Schematic diagram of the experimental setup.

sensitivities in amperes/watt at the two wavelengths) can be determined, the amount of second-harmonic power that had been measured can be calculated. The laser itself, of course, is the ideal source of fundamental radiation against which the second harmonic can be compared. Its relatively high-level output can be accurately measured using a thermopile and then highly attenuated using precisely calibrated attenuators so that the two signals are comparable in strength. Thus, the problem of measuring the second-harmonic power is in effect reduced to a measurement of the ratio of the photomultiplier sensitivity at the second-harmonic wavelength to that at the fundamental, plus an accurate calibration of attenuators at the laser frequency.

The ratio of the sensitivities, which will be denoted by R , was determined using a stable, high-pressure xenon arc lamp, a quartz prism monochromator, and a sensitive thermopile having a relatively fast response time. The basic procedure followed in measuring R is straightforward. The high-intensity xenon lamp, in conjunction with the monochromator, was used as a source of radiation in the regions of 6328 and 3164 Å. Because the arc lamp was intense enough, the sensitive thermopile could be used to make a relative measurement of the powers in the two regions. The signal-to-noise ratio of these measurements was improved by chopping the light at about 40 cps and processing the resulting ac signal from the thermopile with a lock-in amplifier. Next the radiation from the monochromator was strongly attenuated in such a fashion that the intensities in both regions were equally diminished, and the ratio of the responses of the photomultiplier to radiation in the two regions was measured under conditions as similar as possible to those actually encountered in the measurement of the second-harmonic power. The strong neutral attenuation was achieved by defocusing the light source from the entrance slit of the monochromator and by stopping down both the entrance and exit slits. The monochromator slits could be used as neutral attenuators because the power spectrum of the xenon lamp was a smooth curve when viewed through the low-resolution monochromator. This asser-

⁸ R. W. Terhune, P. D. Maker, and C. M. Savage, *Phys. Rev. Letters* **8**, 404 (1962).

⁹ N. Bloembergen and P. S. Pershan, *Phys. Rev.* **128**, 606 (1962).

tion was verified by using the thermopile to measure the ratio of the power transmitted at 6328 Å to that transmitted at 3164 Å for five different total mechanical slit widths. Knowledge of the relative powers in the regions of 3164 and 6328 Å and the relative responses of the photomultiplier to these powers yields the result for R .

In the actual measurement of d_{36} , the RCA-6903 photomultiplier was calibrated both immediately preceding and just after the second-harmonic power generated in the crystal of ADP had been compared with a known amount of fundamental radiation. The result for the ratio of the sensitivities of this particular tube was

$$R = \frac{\text{sensitivity at } 3164 \text{ \AA}}{\text{sensitivity at } 6328 \text{ \AA}} = 9.5 \pm 0.9, \quad (1)$$

where the sensitivities were in units of amperes/watt. In both cases, the response ratio of the photomultiplier was measured with the monochromator slits smaller than the limits of resolution. A glance at the typical spectral sensitivity characteristics for the RCA-6903 is enough to convince one that the corresponding resolution of 2.5 Å at 3164 Å and 50 Å at 6328 Å is adequate to determine an accurate value for R .

The various filters used in the measurement of d_{36} were calibrated in the following ways. The attenuators used to compare the known amount of laser light with the second harmonic were directly calibrated using a thermopile for attenuations of less than 10 dB and a photomultiplier in conjunction with the phase-sensitive detector for larger values. It was also necessary to measure the absorption of second-harmonic radiation by the four CS 7-54 filters which were used to block the laser light from the photomultiplier. This was done by first measuring SHG with four filters in the beam and then with only three.

The second-harmonic power $P_{2\omega}$ generated in a crystal is related to the crystal nonlinearity by Eq. (31) of Ref. 3,

$$P_{2\omega}/P_{\omega}^2 = A\chi^2g. \quad (2)$$

The parameter χ is the generalized nonlinear susceptibility, P_{ω} is the laser power, g is the geometrical factor defined in Eq. (35) of Ref. 3, and the coefficient A is the numerical factor appearing in Eq. (31) of Ref. 3. For crystals of ADP the value of A is 88.5 and in calcite it is 32.2.

The actual measurement of d_{36} was carried out using a crystal of ADP 1.52 cm long. The radius of the collimated laser beam, W , was 0.185 cm. Hence, optimum SHG is obtained with a lens having a focal length of 234 mm; in our measurements a lens having a 250-mm focal length was actually used. The corresponding value for g can be obtained from Fig. 5 of Ref. 3 and was 2.3×10^4 . The measurements of the laser power were made with an Eppley 12-junction thermopile. This

instrument was the standard upon which our absolute measurements were made. It was compared for accuracy with several other thermopiles; all agreed within 1%.

When the entire measurement procedure had been carried out, it was found that for 1.04 mW of laser light incident on the crystal (corresponding to 1.00 mW inside), the second-harmonic power reaching the photomultiplier was $4.8 \times 10^{-11} \text{ W} \pm 30\%$. Taking crystal reflections and filter absorption into account, this corresponds to a total generated second-harmonic power of $7.8 \times 10^{-11} \text{ W} \pm 32\%$. The value of d_{36} is calculated from this data using Eq. (2), with d_{36} substituted for χ . The result is

$$d_{36} = 1.38 \times 10^{-9} \text{ esu} \pm 16\%. \quad (3)$$

This value for d_{36} contains a correction factor of $1/\sqrt{2}$ which is needed because of the enhancement of $P_{2\omega}$ caused by the multimode nature of the laser output.⁴ The magnitude of this correction has been thoroughly investigated and found to be valid for the particular laser used here in measurements carried out by Francois.⁶

The value which we have measured for d_{36} is in excellent agreement with the detailed experiments carried out by Francois using collimated laser beams.⁶ His result is $d_{36} = 1.36 \times 10^{-9} \text{ esu} \pm 12\%$. It must be pointed out that his measurements were carried out using much of the same equipment and some similar techniques; the actual experiments, however, were carried out independently and separated in time by about six months. Thus the results of our measurements are twofold. First, we have shown that the absolute power levels predicted by the calculation of Ref. 3 are correct. Second, we have provided another accurate value of d_{36} in ADP. Except for the work of Francois, previous measurements have yielded results a good deal larger than Eq. (3). McMahon and Franklin⁵ have reported the result $d_{36} = (2.0 \pm 0.5) \times 10^{-9} \text{ esu}$. The result reported for d_{36} in KDP at 1.15 μ by Ashkin, Boyd, and Dziedzic (ABD)⁴ was $(3 \pm 1) \times 10^{-9} \text{ esu}$. ABD pointed out that this result did not incorporate the correction factor for the presence of more than one longitudinal mode in the laser beam. Nevertheless, it is this value which is normally quoted in the literature as the value of d_{36} in KDP. Our measurements indicate that a smaller value would be more appropriate. In particular, the value of d_{36} in KDP at 1.15 μ is estimated to be approximately $1.3 \times 10^{-9} \text{ esu}$ by using our result for d_{36} in ADP at 6328 Å in conjunction with Miller's phenomenological theory,¹⁰ Zernike's refractive index data,¹¹ and the relative measurements of d_{36} (ADP) and d_{36} (KDP) carried out by Miller, *et al.*⁷ Inasmuch as d_{36} (ADP) and d_{36} (KDP) are often taken as standards against which other nonlinearities are compared in relative measurements, these results take on added significance.

¹⁰ R. C. Miller, *Appl. Phys. Letters* **5**, 17 (1964).

¹¹ Frits Zernike, Jr., *J. Opt. Soc. Am.* **54**, 1215 (1964).

III. MEASUREMENTS IN CALCITE

A. Nonlinear Optical Effects in Calcite

The nonlinear optical properties of solids were considered in great detail in the paper of Pershan.¹² The reader is referred to this paper for a more thorough and rigorous discussion of nonlinear optical effects than will be given here. In this section we shall only be concerned with a physical understanding of the various effects which were measured in calcite.

In order to describe the nonlinear optical effects which can occur in a medium, it is convenient to express the induced dipole and quadrupole moments per unit volume as a power series in the electric fields, their gradients, and the magnetic fields present in the medium. Thus, in a *qualitative* fashion we can write

$$\begin{aligned}
 P_i &= \chi_{ij}^{(1)} \mathcal{E}_j + \chi_{ijk}^{(2)} \mathcal{E}_j \mathcal{E}_k \\
 &\quad + \chi_{ijk}^{(3)} \partial_j \mathcal{E}_k + \chi_{ijk}^{(4)} \mathcal{E}_j \nabla \mathcal{C}_k + \chi_{ijkl}^{(5)} \mathcal{E}_j \mathcal{E}_k \mathcal{E}_l \\
 &\quad + \chi_{ijkl}^{(6)} \mathcal{E}_j \partial_k \mathcal{E}_l + \chi_{ijkl}^{(7)} \mathcal{E}_j \mathcal{E}_k \nabla \mathcal{C}_l + \dots, \\
 Q_{ij} &= \eta_{ijk}^{(1)} \mathcal{E}_k + \eta_{ijkl}^{(2)} \mathcal{E}_k \mathcal{E}_l + \dots
 \end{aligned}
 \tag{4}$$

It is stressed that Eq. (4) is far from rigorous; for instance, the χ 's and η 's are actually functions of the frequencies of the various fields with which they are associated. The equation is useful, however, in helping to understand the origin of various nonlinear optical effects and the relationships between them. For instance, the nonlinear susceptibility element $\chi_{ijk}^{(2)}$ is responsible for SHG and for the linear electro-optic effect in crystals such as ADP, KDP, and quartz. In order to display the frequency dependence of $\chi^{(2)}$, the coefficients describing SHG will be written as $\chi_{ijk}^{(2)}(2\omega, \omega, \omega)$ and these are not the same as the coefficients $\chi_{ijk}^{(2)}(\omega, \omega, 0)$ describing the linear electro-optic effect. In a similar fashion, $\chi_{ijkl}^{(5)}(3\omega, \omega, \omega, \omega)$ gives rise to optical third-harmonic generation, $\chi_{ijkl}^{(5)}(2\omega, 0, \omega, \omega)$ to electric-field-induced SHG, and $\chi_{ijkl}^{(5)}(\omega, \omega, 0, 0)$ to the quadratic electro-optic effect.

Calcite belongs to the crystal class $\bar{3}m$; it is a trigonal crystal having a center of inversion. Because of its inversion symmetry the coefficients $\chi^{(2)}$, $\chi^{(3)}$, $\chi^{(7)}$, and $\eta^{(1)}$ in Eq. (4) are all required to be zero. Thus, the largest nonlinear effects in calcite are of one higher order nonlinearity than are the effects in noncentrosymmetric crystals. In calcite, Eq. (4) takes the form

$$\begin{aligned}
 P_i &= \chi_{ij}^{(1)} \mathcal{E}_j + \chi_{ijk}^{(4)} \mathcal{E}_j \nabla \mathcal{C}_k + \chi_{ijkl}^{(5)} \mathcal{E}_j \mathcal{E}_k \mathcal{E}_l \\
 &\quad + \chi_{ijkl}^{(6)} \mathcal{E}_j \partial_k \mathcal{E}_l + \dots, \\
 Q_{ij} &= \eta_{ijkl}^{(2)} \mathcal{E}_k \mathcal{E}_l + \dots
 \end{aligned}
 \tag{5}$$

There are two separate types of SHG in calcite on which we will focus our attention. The first can be referred to as quadrupole-type SHG (QSHG). Pershan¹² has shown that for the case of SHG the effects arising from $\chi^{(4)}$, $\chi^{(6)}$, and $\eta^{(2)}$ can be combined and can be represented as occurring because of the presence of an

TABLE I. The general form of χ_{ijkl} (or η_{ijkl}) for the crystal class $\bar{3}m$.

	xx	yy	zz	yz	zy	xz	zx	xy	yx
xx	χ_{11}	χ_{12}	χ_{13}	χ_{14}	χ_{15}				
yy	χ_{12}	χ_{11}	χ_{13}	$-\chi_{14}$	$-\chi_{15}$				
zz	χ_{31}	χ_{31}	χ_{33}						
yz	χ_{41}	$-\chi_{41}$		χ_{44}	χ_{45}				
zy	χ_{51}	$-\chi_{51}$		χ_{54}	χ_{55}				
xz						χ_{44}	χ_{45}	χ_{41}	χ_{41}
zx						χ_{54}	χ_{55}	χ_{51}	χ_{51}
xy								$\frac{\chi_{11}-\chi_{12}}{2}$	$\frac{\chi_{11}-\chi_{12}}{2}$
yx								$\frac{\chi_{11}-\chi_{12}}{2}$	$\frac{\chi_{11}-\chi_{12}}{2}$

effective quadrupole moment at the second-harmonic frequency. Thus QSHG can be described by an equation of the form

$$p_i(2\omega) = \eta_{ijkl}(2\omega, \omega, \omega) \mathcal{E}_k(\omega) \mathcal{E}_l(\omega).
 \tag{6}$$

The subscripts refer to the crystallographic axes, and $q_{ij}(2\omega)$ and $\mathcal{E}_k(\omega)$ are the space-dependent amplitudes of the quadrupole moment and the optical electric field having a time dependence of $e^{-i2\omega t}$ and $e^{-i\omega t}$, respectively. Additional SHG can be induced in calcite by applying a dc electric field to the crystal. It can be said that the application of the biasing electric field upsets the center-of-symmetry of the crystal and allows normal dipolar SHG to occur. This effect is referred to as electric-field-induced SHG (or ESHG). The space-dependent amplitude of the dipole moment per unit volume induced at the second-harmonic frequency is

$$p_i(2\omega) = \chi_{ijkl}(2\omega, 0, \omega, \omega) \mathcal{E}_j(0) \mathcal{E}_k(\omega) \mathcal{E}_l(\omega).
 \tag{7}$$

The general form for a fourth-rank tensor χ_{ijkl} (or η_{ijkl}) describing an effect in a crystal having the symmetry $\bar{3}m$ is shown in Table I. The tensors in which we are interested reflect the symmetry of the effects which they describe as well as the symmetry of calcite. Thus the tensor $\chi_{ijkl}(2\omega, 0, \omega, \omega)$ in Eq. (7) is symmetric in its last two indices and the tensor $\eta_{ijkl}(2\omega, \omega, \omega)$ in Eq. (6) is symmetric in both its first and last pair of indices. Using Eqs. (6) and (7) and the correct forms for the relevant tensors, the second-harmonic power obtained will be calculated for the particular experimental situation which we used.

B. Calculation of the Second-Harmonic Power

In carrying out this calculation the same techniques employed in Ref. 3 will be used. The equation for the second-harmonic electric field can be written as¹²

$$\begin{aligned}
 \nabla \times \nabla \times \mathbf{E}(2\omega) &= \frac{4\omega^2}{c^2} (1 + 4\pi\chi) \cdot \mathbf{E}(2\omega) \\
 &= \frac{16\pi\omega^2}{c^2} \{ \mathbf{p}(2\omega) - \nabla \cdot \mathbf{q}(2\omega) \}.
 \end{aligned}
 \tag{8}$$

¹² P. S. Pershan, Phys. Rev. **130**, 919 (1963).

The importance of this equation is that it shows that the source driving $\mathbf{E}(2\omega)$ is $\mathbf{p}(2\omega) - \nabla \cdot \mathbf{q}(2\omega)$. The calculations of Ref. 3 were carried out for a polarization driving source and hence the results of those calculations must be slightly modified when applied to calcite.

In our experiments the focused laser beam passed through the crystal as an ordinary wave linearly polarized along the crystal Y axis (the axis lying in a mirror plane¹³). When measuring ESHG, the dc electric field E_{dc} was applied along the same axis. The z axis of our coordinate system is chosen as the axis of the laser beam, and the y axis is the same as the Y axis of the crystal. Since index matching was used, only the component of the driving source along \hat{U} , the unit vector specifying the polarization of the free extraordinary wave at 2ω , is effective in SHG. In calculating the driving source, the transverse spatial derivatives are neglected with respect to the longitudinal derivatives because $\partial E^2(\omega)/\partial x \approx \partial E^2(\omega)/\partial y \approx (2/k_1 w_0) \partial E^2(\omega)/\partial z$ and $2/k_1 w_0 \ll 1$. The parameter k_1 is the magnitude of the propagation vector of the ordinary light at ω , and w_0 is the radius of the laser-beam focal spot. In the same approximation we have $\partial E^2(\omega)/\partial z = 2ik_1 E^2(\omega)$. The resulting driving source is

$$\hat{U} \cdot [\mathbf{p}(2\omega) - \nabla \cdot \mathbf{q}(2\omega)] = -(\chi_{51} E_{dc} + 2ik_1 \eta_{\text{eff}}) \sin^2(\theta_m + \alpha) E^2(\omega), \quad (9)$$

where

$$\eta_{\text{eff}} = \eta_{13} \cos \theta_m - \eta_{12} \sin \theta_m \cot(\theta_m + \alpha). \quad (10)$$

The index-matching angle is θ_m and α is the double refraction angle. The analysis of Ref. 3 can be used to find $\mathbf{E}(2\omega)$ with χ replaced by $-(\chi_{51} E_{dc} + 2ik_1 \eta_{\text{eff}})$. Thus $\mathbf{E}(2\omega)$ is given by Eq. (27) of that reference when the correct substitution is made for χ .

In proceeding further, however, caution must be exercised. The reason for this is that in order to calculate the second-harmonic power generated in calcite the correct form of the Poynting's vector must be used to include the presence of the quadrupole moment at 2ω . Pershan¹² has shown that the correct Poynting's vector is given as

$$\mathbf{S} = \frac{c}{4\pi} \mathbf{E} \times \mathbf{H} - \mathbf{E} \cdot \frac{\partial}{\partial t} \mathbf{Q}, \quad (11)$$

where the various fields are now time variables, not space-dependent amplitudes. The correction terms involving the quadrupole moment can be understood by realizing that electrical currents are associated with a quadrupole moment which is changing with time, and the interaction of these currents with the electric fields represent a flow of energy through the medium. The presence of this correction term greatly complicates the exact evaluation of $P_{2\omega}$. Qualitative understanding of

the effects of the correction term can be obtained by considering the simple plane-wave problem.

Consider a plane-wave laser beam propagating through calcite with the slight mismatch Δk . The solution for $E(2\omega)$ is obtained from Eq. (19) of Ref. 3; the result is substituted into Eq. (11) which is then averaged over time. One obtains

$$\hat{z} \cdot \mathbf{S} = A \left[4k_1^2 \eta_{\text{eff}}^2 + \chi_{51}^2 E_{dc}^2 - \frac{2\eta_{\text{eff}} \chi_{51} E_{dc}}{\sin(\theta_m + \alpha)} \frac{1}{z'} \right. \\ \left. \times \left(\frac{\sin \frac{1}{2} \Delta k z'}{\frac{1}{2} \Delta k z'} \right)^{-1} - \frac{4k_1 \eta_{\text{eff}}^2}{\sin(\theta_m + \alpha)} \frac{1}{z'} \left(\frac{\sin \frac{1}{2} \Delta k z'}{\frac{1}{2} \Delta k z'} \right)^{-2} \right. \\ \left. \times \frac{1 - \cos \Delta k z'}{\Delta k z'} \right], \quad (12)$$

where

$$A = \frac{2\pi\omega^2}{n_1^2 c} E_{\omega}^4 \frac{\sin^2(\theta_m + \alpha)}{\cos^2 \alpha} z'^2 \left(\frac{\sin \frac{1}{2} \Delta k z'}{\frac{1}{2} \Delta k z'} \right)^2,$$

n_1^0 is the index of refraction for the laser beam, and z' is the distance from the entrance face of the crystal. The last two terms of Eq. (12) occur because of the quadrupole correction to the Poynting's vector, and their importance increases as Δk increases. Using the experimentally measured relation $2k_1 \eta_{\text{eff}} \approx 140 \chi_{51}$, estimate shows that for propagation at the beam divergence angle to the index-matching direction (under conditions of optimum focusing) the correction terms are smaller than the normal terms, but not necessarily small enough that they are negligible. Thus, for an actual laser beam, which is composed of many plane-wave components, one might expect to see some effects due to the quadrupole correction. Also, these effects should increase as the beam is more strongly focused.

It is expected, however, that the first two terms of Eq. (12) will describe the dominant behavior of SHG in calcite. The correction terms may or may not be evident as slight modifications to this behavior. Thus Eq. (2) will be used to describe SHG in calcite unless experiments should indicate otherwise. Of course, χ^2 must be replaced by $\chi\chi^*$ and the correct substitution made for χ .

C. Equipment

Because the second-harmonic power generated in calcite is on the order of 10^{-6} of that generated by a comparable crystal of ADP, much of the equipment used in these measurements was different from that previously described. The laser was a Spectra-Physics model 125 He-Ne laser operating at 6328 Å and having a usable output of approximately 50 mW. The output beam of the laser was collimated by the output mirror. Even with the more powerful laser the SHG in calcite was still several orders of magnitude smaller than that

¹³ Standards on Piezoelectric Crystals, Proc. IRE 37, 1378 (1949).

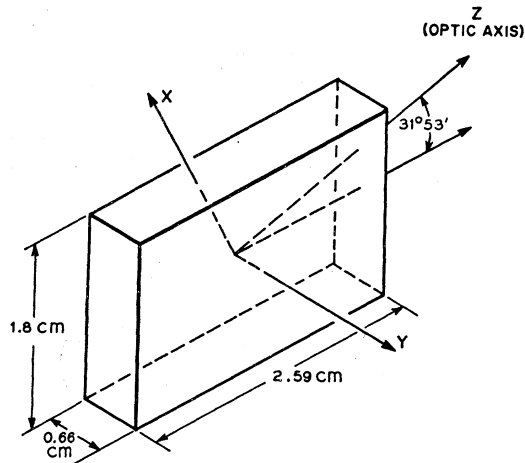


FIG. 2. Orientation and dimensions of the calcite crystal used in the measurements.

previously detected from ADP. For this reason an RCA-1P28 photomultiplier cooled to liquid nitrogen temperature, -195.8°C , was used as the detector. When the cathode was well shielded from light, its dark current, as viewed with an oscilloscope, was on the order of tens of electrons per second; this response corresponds to an incident second-harmonic power of about 2×10^{-17} W.

The crystal used in these experiments was of highest optical quality and was cut with the orientation and dimensions shown in Fig. 2; it was polished on all six sides. All faces were flat to within two wavelengths and opposite faces were parallel to better than 5 min., the entrance and exit faces to better than 30 sec. The Y axis was within 1° of being perpendicular to the large faces. The optic axis was oriented so that at index-matching the laser beam would be nearly normal to the entrance and exit faces.

The large electric fields required to measure ESHG were applied along the Y axis of the crystal. In order to make the applied field as homogeneous as possible flat copper electrodes 3.2 cm square, larger than the largest faces of the crystal, were used. They were incorporated into a plexiglas crystal holder and were applied directly to the crystal which was held in place with a small amount of pressure. In order to prevent breakdown around the crystal when measuring ESHG it was immersed in G.E. SF-97(100) silicone dielectric fluid which is nearly transparent to the second-harmonic radiation. The crystal was mounted so that it could be rotated around its Y axis, and its angular position could be controlled to better than 0.05 deg.

The measurements in calcite were carried out in a *relative* fashion; that is, the SHG from calcite was compared with SHG from ADP and the value of the nonlinearity in calcite was computed relative to d_{36} . This approach was more accurate than a direct absolute measurement.

D. Measurement of QSHG

Measurements of quadrupole-type SHG were carried out with the crystal mounted in air. The actual experimental procedure was straightforward. First QSHG was measured under conditions of optimum focusing. Then, after several measurements were taken, the procedure was repeated with the laser beam attenuated and unfocused in a crystal of ADP. Direct comparison of the detected second-harmonic powers yielded the value of the quadrupole-type nonlinearity in terms of d_{36} .

An actual experimental curve of the variation of the quadrupole-type second-harmonic power as the calcite crystal was rotated through the index-matching direction is shown in Fig. 3. The width of the curve corresponds very nearly to the divergence angle of the focused light. The curve was made using a chart recorder driven by the lock-in amplifier as the crystal was slowly rotated by a synchronous motor. The zero line corresponding to zero QSHG does not correspond to zero signal, for there was a background signal associated with the laser beam. As shown, when the laser beam was blocked the signal disappeared. There are several possible explanations for the background radiation. It could be due to SHG at the crystal surfaces, SHG at any of the other surfaces through which the laser beam passed, or to a slight amount of laser tube fluorescence in the region of 3164 \AA transmitted by the 6328 \AA interference filter which was used at the laser output. The signal was not due to radiation at 6328 \AA , as the addition of extra CS7-54 filters did not change its level. The exact origin of the background signal was not

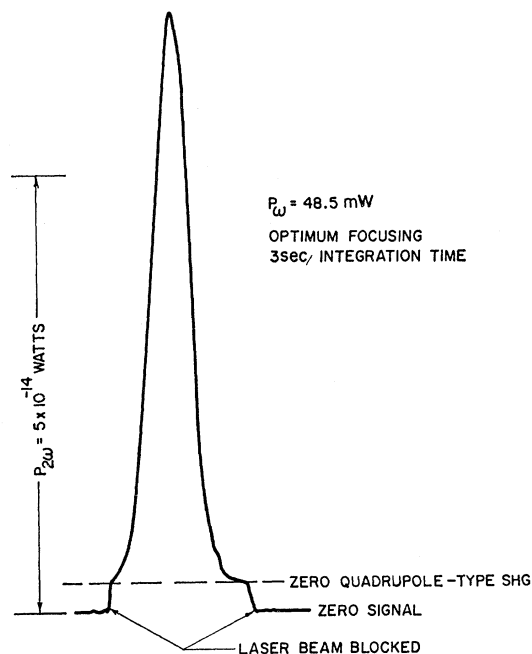


FIG. 3. The variation of the quadrupole-type SHG as the calcite crystal was rotated through the index-matching direction.

determined and in measuring QSHG it was simply subtracted from the total signal.

The correction terms due to the modified Poynting's vector displayed in Eq. (12) were neglected. It will be shown later that the neglect of these corrections adds an uncertainty of only several percent. Inasmuch as the estimated probable error in the measurements was quite a bit larger, this uncertainty makes little difference.

The major experimental difficulty was in achieving optimum focusing when measuring SHG in calcite. The reason for this was that a 3-sec integration time was used on the lock-in amplifier. Consequently there was a relatively long delay between the time an adjustment was made and the time that the results of the change became apparent. The problem was compounded by the fact that some adjustments could not be made independently of one another. Using experience as our guide, it was felt that the lens position could be adjusted to give within 5% of the maximum second-harmonic power. The other major probable errors occurred in accounting for the reflection losses introduced by the lens and the crystal faces.

Two experimental runs were made using a 250-mm lens to focus the laser beam which had a radius $W = 0.142$ cm into the calcite crystal. The result was optimum focusing, $w_0 = 3.5 \times 10^{-3}$ cm and $g = 8 \times 10^3$. For the measurements in the 1.52-cm ADP crystal we had $w_0 = W$ and $g = 115$. The SHG from calcite was observed using about 50 mW of laser power, and it was about 0.01 of that observed from ADP using at most a 5-mW laser beam. The results were in excellent agreement and the average of them is

$$2k_1\eta_{\text{eff}}/d_{36} = (2.8 \pm 0.4) \times 10^{-8}, \quad (13)$$

or

$$\eta_{\text{eff}}/d_{36} = (0.85 \pm 0.12) \times 10^{-8}. \quad (14)$$

Using ruby lasers, the best estimate of TMS⁸ for a nonlinearity similar to the one given by Eq. (14) was about 3×10^{-8} . It is interesting to note that since QSHG is one higher order nonlinearity than normal SHG, one would expect that its nonlinearity coefficient would be on the order of $k_1 a_0$ smaller, where a_0 is a typical atomic dimension. Since $a_0 \approx 1 \text{ \AA}$, we have $k_1 a_0 \approx 10^{-8}$ which is in good order-of-magnitude agreement with Eq. (13).

E. Measurement of θ_m

An accurate measurement of the index-matching angle θ_m was carried out by observing QSHG with the crystal mounted in air. The measurements were carried out under conditions of optimum focusing. For this case there was no need to differentiate between the "nominal" and "optimum" index-matching directions defined by Kleinman, Ashkin, and Boyd.¹⁴ For instance, the parameter β defined in Ref. 14 was approximately

33 and the calculated difference between the two directions is only 4 sec for an infinitely long crystal. For our crystal the difference would be even smaller.

The measurements were carried out in two steps. First, the index-matching direction was located with respect to the normal to the incident face by observing the position at which maximum QSHG was obtained. Then, the optic axis was located with respect to the same normal by observing the interference figure of the calcite crystal when placed in converging laser light between crossed polarizers. These measurements made it a simple matter to calculate θ_m . Experimental accuracy was determined by the degree to which the crystal could be positioned, namely to ± 0.05 deg. The measured value was

$$\theta_m = 29^\circ 36' \pm 9'. \quad (15)$$

This value agrees very well with the value $\theta_m = 29^\circ 35' \pm 10'$ which was calculated using values for the indices of refraction obtained from curves which were carefully plotted using data available from standard sources.

F. Measurement of ESHG

The measurements of the nonlinearity for ESHG were also carried out in a relative fashion. By measuring the total SHG as a function of the applied electric field and using the power generated with zero field as a reference, the value of χ_{51} was calculated in terms of $2k_1\eta_{\text{eff}}$. This method for determining χ_{51} was adopted because it was the most direct measurement and also the most accurate.

The major experimental difficulty encountered in these measurements was an apparent slow build-up of charge at the crystal surfaces which tended to neutralize the applied dc electric field. It is conjectured that this build-up occurred because of charge migration in the crystal and non-Ohmic contact between the crystal and the electrodes. No attempts were made at making the contact Ohmic; in fact, a slight amount of dielectric fluid was inserted between the crystal face and the electrode. This was done in order to eliminate pitting of the calcite faces which had been observed in earlier measurements carried out with another crystal and which probably was due to nonuniformities between the two surfaces. There were two reasons for suspecting the presence of charge build-up. They were a non-repeatability of SHG obtained with zero applied voltage and a departure of the dependence of $P_{2\omega}$ upon E_{dc} from quadratic. In the first case, it was found that the second-harmonic power generated with zero applied voltage depended upon when the measurement was made. If it had been a long time since voltage had last been applied to the crystal, then the power readings were consistent with other readings made under similar conditions. On the other hand, if a measurement were made just after a voltage which had been applied for a long time was removed, the power would be consider-

¹⁴ D. A. Kleinman, A. Ashkin, and G. D. Boyd, Phys. Rev. 145, 338 (1966).

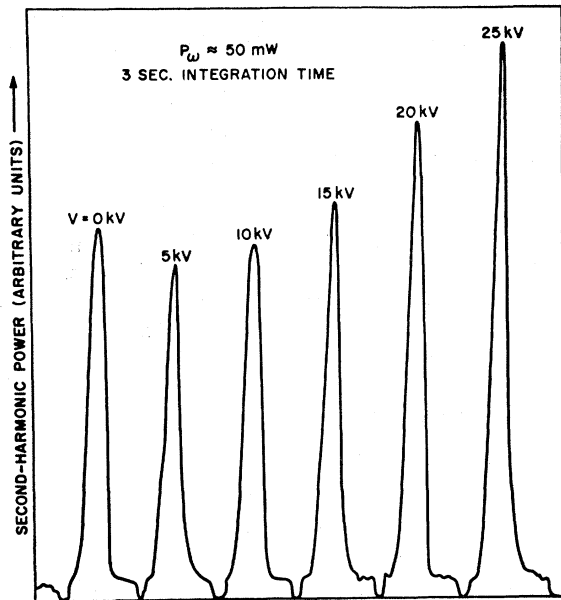


FIG. 4. Measurement of SHG in calcite for various applied voltages. The crystal is rotated through the index-matching direction for each voltage.

ably greater. In other words, it appeared as if an internal electric field had been induced in the crystal. In the second case, it was found that the second-harmonic power varied less rapidly than E_{dc}^2 . Both of these phenomena can be explained by the electric fields developed by the build-up of charge at the surfaces. In addition, if voltages were held constant over extended periods of time, the build-up of charge could be observed by recording the slow decrease in second-harmonic power. An estimate of the associated decay time would be on the order of 10 min.

Inasmuch as the effects of charge build-up could not adequately be described, the experiments were carried out in such a way that they were minimal. In particular, measurements of $P_{2\omega}$ as a function of the applied voltage were always made with either monotonically increasing or decreasing voltages, usually starting with zero voltage. An example of an actual experimental chart is shown in Fig. 4. These curves were recorded by rotating the crystal through the index-matching angle for each value of the applied voltage. The advantage of this method is that the true zero-SHG level can be accurately determined for each curve. The background signal can thus be eliminated. The dips between the curves occurred when the laser beam was blocked during measurement of its power and they correspond to zero signal. In an alternative method of measurement the crystal orientation was fixed and only the voltage was changed. The results obtained using either method were equally good.

The results of the measurements are shown in Figs. 5, 6, and 7 where the parabolic curves of $P_{2\omega}$ as a function of the applied voltage are plotted. The parameters

of the parabolas were chosen to give a good fit with the experimental points. Inasmuch as the voltage applied to the electrodes could not be reversed, the points in Fig. 7 were obtained by rotating the crystal between the electrodes by 180° using the laser beam as the axis of rotation. It can be shown that the effects of this change are the same as would be obtained by applying a negative voltage to the crystal; namely, the phase of the second-harmonic electric field radiated by the electric-field-induced effect relative to the phase of the field radiated by the quadrupole effect is changed by 180° . In each of the three figures the minimum of the parabolic curve occurs for nonzero values of the applied fields. This phenomenon was seen directly in Fig. 4 where the second-harmonic powers obtained with 5 kV and 10 kV applied to the crystal were less than that obtained with no applied voltage. The curves of $P_{2\omega}$ as a function of the applied voltage V are parabolas displaced from the $V=0$ axis; they can be written as

$$P_{2\omega} = P_0' + \beta(V - V_0)^2 \tag{16}$$

$$= (P_0' + \beta V_0^2) + \beta V^2 - 2\beta V_0 V, \tag{17}$$

where V_0 is the amount by which the curve is shifted and P_0' is the minimum $P_{2\omega}$. The difference between the power obtained with no applied field and P_0' is $\Delta P_{2\omega} = \beta V_0^2$. The displacement of the curves is not due to the build-up of charge at the crystal surfaces.

Terhune, Maker, and Savage⁸ were the first to observe the displacement of the parabolic curves. They explained the shift as occurring because of SHG at the surfaces of the crystal coherent with the ESHG in the bulk of the crystal. A more detailed analysis of the problem was carried out by Bloembergen and Pershan (BP).⁹ They showed that the boundary second-harmonic wave caused by the presence of the electric-field-induced effect could interfere with the bulk quadrupole

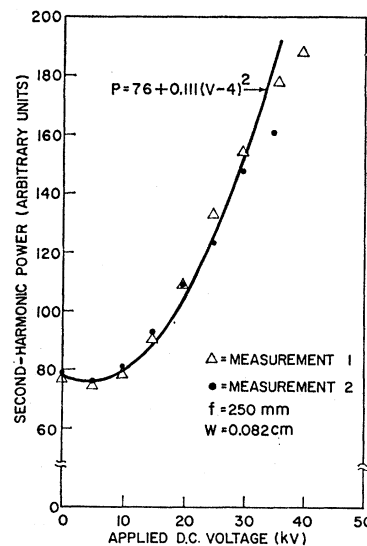


FIG. 5. SHG in calcite as a function of the voltage applied to the 0.66-cm-thick crystal. The parameters of the parabolic curve were chosen to give a good fit with the experimentally measured points.

field and bring about a displacement of the parabolic curves. This interference is explicitly displayed by their Eq. (4.19). However, BP point out that such effects only occur when a homogeneous field is applied only over a part of the laser beam's path through the crystal or, in a more generalized sense, when the applied electric fields are inhomogeneous. These conditions are compatible with the geometry used in the experiments of TMS where the applied electric field was highly non-uniform and did not occupy the entire crystal. For our experiments, however, care was taken to produce a nearly homogeneous field throughout the entire crystal. Nevertheless, the magnitudes of the curve shifts measured in our experiments were approximately the same as those measured by TMS.¹⁵ This result is a strong argument against attributing the shift of the parabolic curves to inhomogeneous fields.

There are several other possible explanations for the curve shift which we will briefly discuss:

(1) Suppose that the background signal which we detected in our experiments was second-harmonic-power generated externally to the calcite crystal. This could occur, for instance, in filters, windows, or the dielectric fluid. If a portion of this field was in phase with the bulk ESHG field created in the calcite crystal, then the two fields could interfere and the total second-harmonic power could be written in the form of Eq. (16). Also, $\Delta P_{2\omega}$ would be less than or equal to the total background power. In some of our measurements, however, $\Delta P_{2\omega}$ was considerably greater than the background signal.

(2) The curve shifts could also be explained by assuming that χ_{51} or η_{eff} , or both of them, are complex and not purely real quantities. In this case the quadrupole and the electric-field-induced second-harmonic fields would not necessarily be 90° out of phase (in time) and

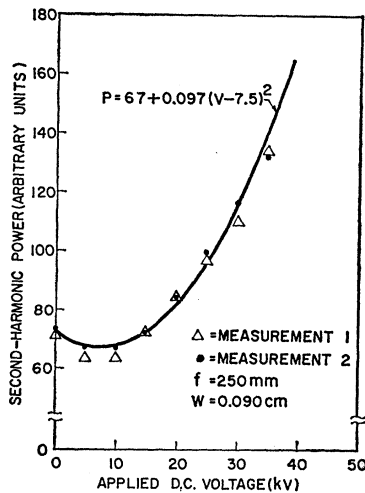


FIG. 6. SHG in calcite as a function of the voltage applied to the 0.66-cm-thick crystal. The parameters of the parabolic curve were chosen to give a good fit with the experimentally measured points.

¹⁵ P. D. Maker (private communication).

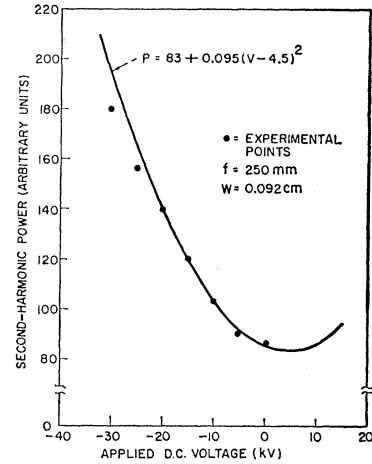


FIG. 7. SHG in calcite as a function of the voltage applied to the 0.66-cm-thick crystal. The parameters of the parabolic curve were chosen to give a good fit with the experimentally measured points.

they could interfere with each other. The second-harmonic power could be written in the form of Eq. (17).

Note added in proof. Lee, Chang, and Bloembergen, Phys. Rev. Letters 18, 167 (1967) recently have measured a similar curve shift in nonlinear electroreflectance which also might be explained by complex nonlinear susceptibilities.

(3) The shift of the parabolic curves could also be due to the quadrupole correction to the Poynting's vector discussed in Sec. IIIB. The consequences of this correction for a plane-wave laser beam were displayed in Eq. (12) which is of the form of Eq. (17). It is clear that the values of $\Delta P_{2\omega}$ and V_0 are determined by Δk and z' . For an actual focused laser beam the complete solution must account for all the plane-wave components which make up the real beam. Thus, one would expect the parameters $\Delta P_{2\omega}$ and V_0 to be determined by δ , the divergence angle of the focused beam. As a result, the shift of the parabola would depend upon the degree to which the beam was focused and, in particular, the curve shift would increase as the beam was focused harder. Experimental evidence for this dependence of V_0 upon focusing was inconsistent. Such inconsistency is not entirely unexpected, however, as optimum positioning of the lens was rather difficult due to the low powers being measured. The consequent variations in lens positioning would undoubtedly also have an effect on the shift of the curves.

Unfortunately it was not possible to determine in our experiments which of these explanations, if any, was responsible for the curve shifts which we measured. With higher power cw lasers it should be possible to investigate the dependence of the curve shift upon various factors and, hopefully, to determine its cause.

In Sec. IIID the parameter $2k\eta_{eff}$ was calculated from the second-harmonic power measured with no field applied to the crystal. However, the preceding discussion has shown that the zero-field power may not correspond to pure QSHG. In the same fashion, the

parabola minimum may not be pure QSHG either. Thus, there is an uncertainty of approximately $\Delta P_{2\omega}$ in our measurement of the quadrupole second-harmonic power. Fortunately $\Delta P_{2\omega}$ was always less than 8% of the power obtained with no applied field. Thus, in neglecting the appropriate corrections, less than 4% error was introduced into the measured value for $2k_{1\eta_{eff}}$.

The measured value of χ_{51} is easily determined from the curves in Figs. 5, 6, and 7. This is done by finding that value of $\Delta V \equiv V - V_0$ for which the ESHG is equal to the QSHG, taken to be the SHG measured with no field applied to the crystal. The average of these values is $(\Delta V)_{av} = 27 \text{ kV} \pm 10\%$. This corresponds to an applied electric field $(\Delta E)_{av} = 42 \text{ kV/cm} \pm 10\%$. The measured value for χ_{51} is

$$\chi_{51}/2k_{1\eta_{eff}} = 0.73 \times 10^{-2} \pm 10\%, \quad (18)$$

or

$$\chi_{51}/d_{36} = 2.1 \times 10^{-5} \pm 24\%. \quad (19)$$

This result is in excellent agreement with the results given by TMS⁸ and by Maker and Terhune.¹⁶ Their estimate for a different nonlinearity element was $3 \times 10^{-5} d_{36}$.

G. Measurement of the Electric-Field-Induced Birefringence

Experiments were also carried out to make a measurement of the birefringence induced in calcite by the application of an electric field. Circularly polarized light was passed through the crystal along its optic axis and the change in its ellipticity due to the applied field was measured. The ac electric field was applied along the *Y* axis of the crystal, an analyzer prism was oriented at 45° to the *X* and *Y* axes, and the changes in ellipticity were detected as an amplitude modulation of the light.

The induced birefringence in calcite depends quadratically upon the applied electric field but in our measurements it cannot be attributed solely to the quadratic-electric-optic effect. A similar induced birefringence can also be produced by the combined effect of photoelasticity and stresses induced in the crystal which are proportional to the square of the electric

field. Such stresses arise due to electrostriction and due to the force exerted on the electrodes, and hence the crystal, by the electric field. Stresses which depend linearly upon the electric field do not occur because of calcite's inversion symmetry. In our experiments it was not possible to distinguish between the various effects. For this reason we use the coefficient β to relate the induced birefringence to the applied electric field; the expression is

$$\Delta n = (2\pi/n_0)\beta E_{dc}^2. \quad (20)$$

If the effects of photoelasticity are neglected then β is given as the difference between the appropriate nonlinear susceptibility elements, $\chi_{11}(\omega, \omega, 0, 0) - \chi_{12}(\omega, \omega, 0, 0)$.

The induced birefringence was very small, the modulation of the light being only about 0.02% for an applied electric field of 60 kV/cm peak-to-peak. A lock-in amplifier was used to detect the signal. The result of our measurements was

$$|\beta| = 2.0 \times 10^{-14} \text{ esu} \pm 16\%. \quad (21)$$

As a comparison, the Kerr coefficient of nitrobenzene is 3×10^{-10} esu; crystalline BaTiO₃ exhibits one of the largest solid-state Kerr effects and its Kerr coefficient is about 3×10^{-12} esu at room temperature.¹⁷

IV. CONCLUSION

We have made an accurate absolute measurement of d_{36} in ADP and accurate relative measurements of quadrupole-type SHG and electric-field-induced SHG in calcite. All measurements were made using optimally focused cw gas-laser beams. The measurements in ADP show that focused beams can be employed to carry out accurate measurements of crystal nonlinearities. The experiments in which the higher order nonlinearities in calcite were measured demonstrate a practical application of the power enhancements available from focusing.

ACKNOWLEDGMENTS

The authors are indebted to Dr. A. Ashkin for his critical reading of the manuscript and the assistance of R. Griffin, who oriented, cut, and polished the crystals, is gratefully acknowledged.

¹⁶ P. D. Maker and R. W. Terhune, Phys. Rev. **137**, A801 (1965).

¹⁷ J. E. Geusic, S. K. Kurtz, T. J. Nelson, and S. H. Wemple, Appl. Phys. Letters **2**, 185 (1963).